ISBN: 978-3-95450-218-9 ISSN: 2226-0374 doi:10.18429/JACoW-COOL2019-TUY02

PROGRESS IN MUON IONIZATION COOLING DEMONSTRATION WITH MICE*

D. M. Kaplan†, Illinois Institute of Technology, Chicago, IL 60616 USA
K. Long, Imperial College London, London SW7 2AZ, UK

on behalf of the MICE collaboration

Abstract

The Muon Ionization Cooling Experiment (MICE) at RAL has collected extensive data to study the ionization cooling of muons. Several million individual particle tracks have been recorded passing through a series of focusing magnets in a number of different configurations and a liquid-hydrogen, lithium-hydride, or polyethylene-wedge absorber. Via measurement of the tracks upstream and downstream of the absorber, we have observed ionization cooling. Our measurement is in good agreement with our simulation of the effect. Further studies are now providing more and deeper insight.

INTRODUCTION

High-energy lepton colliders have been proposed as potential future facilities to follow up on discoveries made and to be made at the LHC. The design of such machines is strongly influenced by radiative effects (synchrotron radiation and beamstrahlung). Since these scale with the fourth power of lepton mass, the use of the muon rather than the electron would substantially suppress them. Muon colliders can thus employ rings of small circumference for acceleration and collisions, reducing facility footprints and construction and operating costs. Muons likewise give more-monochromatic collisions and allow much higher energies (10 TeV or more) [1,2] than do electrons. Moreover, the coupling of the Higgs field to leptons being proportional to the square of lepton mass, the muon collider has the unique ability to produce the Higgs boson exclusively, in the *s* channel. This, along with the highly precise muon beam energy spread and calibration ($\Delta E/E \lesssim 10^{-5}$), enables a direct measurement of the Higgs mass and width [3]. While it complicates beam handling, muon decay (mean lifetime = 2.2 μs) enables stored-muon-beam neutrino factories—the most capable technique yet devised for precision measurements of neutrino oscillation and searches for new physics in the neutrino sector [4-10].

Figure 1 compares muon collider and neutrino factory schematic layouts. Two muon-production approaches are under consideration: via pion production and decay, or via $e^+e^- \rightarrow \mu^+\mu^-$ just above threshold (in a positron storage ring with internal target)—the Low EMittance Muon Accelerator, or LEMMA [11]. While potentially bypassing the need for muon cooling, the LEMMA approach itself has significant technical challenges to overcome if the desired high $\mu^+\mu^-$ luminosity ($\geq 10^{34}$ cm^{-2} s^{-1}) is to be achieved; it also produces insufficient muons for use as a neutrino factory.

* Work supported by STFC
† kaplan@iit.edu

If the pion-production approach is chosen, the facility performance and cost depend on the degree to which a muon beam can be cooled. The desired emittance reduction factor for a neutrino factory is $\mathcal{O}(10–100)$, with 4D transverse cooling sufficing, while that for a muon collider is $\mathcal{O}(10^6)$, and 6D cooling is required [12,13].

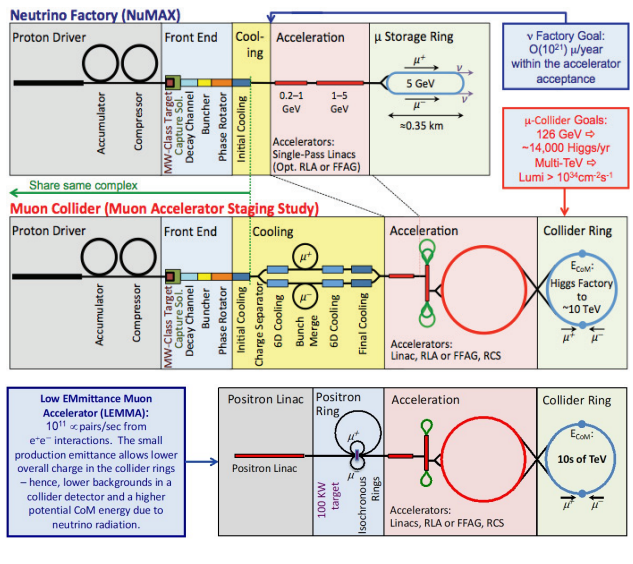

Figure 1: Schematic layouts of possible muon accelerator facilities: (top) neutrino factory; (center) muon collider, employing pion production and decay; and (bottom) employing $\mu^+\mu^-$ pair production in fixed-target e^+e^- collisions (LEMMA).

IONIZATION COOLING

Established methods of particle-beam cooling (electron, laser, stochastic, and synchrotron-radiation cooling) are ineffective for the muon due to its short lifetime, large mass, and lack of internal substructure, thus non-traditional approaches are required. Only one cooling mechanism —ionization cooling[1] [14-19] — works on muons in microseconds, allowing small enough emittances to be reached with $\mathcal{O}(10^{-2\pm1})$ muon survival. Moreover, like electron cooling, ionization cooling was first proposed at the Budker Institute of Nuclear Physics (BINP). Thus it is fitting that we report here at BINP at the COOL'19 Workshop on the progress of its experimental demonstration.

[1] Essentially a form of electron cooling, but with an electron density many orders of magnitude larger than is possible in an electron beam.

ISBN: 978-3-95450-218-9 ISSN: 2226-0374 doi:10.18429/JACoW-COOL2019-TUY02

In ionization cooling, muons traverse a series of energy absorbers, of low atomic number, in a focusing magnetic lattice, with normalized transverse emittance evolving according to [16-19]

$$\frac{d\varepsilon_n}{ds} \approx \frac{-1}{\beta^2}\left\langle \frac{dE_\mu}{dx}\right\rangle \frac{\varepsilon_n}{E_\mu} + \frac{\beta_\perp (13.6\,\mathrm{MeV})^2}{2\beta^3 E_\mu m_\mu c^2 X_0}. \quad (1)$$

Here βc is the muon velocity, $\beta_\perp$ the lattice betatron function at the absorber, $\langle dE_\mu/ds\rangle$ the mean energy loss per unit length, m_μ the muon mass, and X_0 the absorber radiation length. ($\beta_\perp$ takes the place of the more usual β_x or β_y when cylindrically symmetric solenoidal focusing is used; thus we have here $\beta_x = \beta_y \equiv \beta_\perp$, with cooling equal in the x-x' and y-y' phase planes.) To allow repeated cooling, absorbers are interspersed with accelerating cavities.

In Eq. 1, the first term describes cooling, and the second, heating due to multiple Coulomb scattering.[2] To minimize the heating term, small $\beta_\perp$ (strong focusing) and large X_0 (low-Z absorber material) are employed. For a given cooling-channel design, cooling proceeds towards an equilibrium emittance value at which the heating and cooling terms balance. Once equilibrium is reached, continued cooling requires a revised design with lower $\beta_\perp$. Ionization cooling works optimally near ≈ 200 MeV/c momentum [16-19], at which the dE/dx energy loss rate in matter is (counterintuitively) near its minimum [20] (see Fig. 2). This reflects the trade-off between heating effects of "straggling" at higher momenta and the negative slope of the dE/dx curve at momenta below the minimum (leading to problematic, positive feedback for energy-loss fluctuations).

Emittance Exchange

Ionization cooling as just described is a purely transverse effect. In the longitudinal phase plane it tends to heat the beam due to the negative dE/dx slope. While longitudinal cooling might appear to be feasible by operating at somewhat higher momentum, where the dE/dx slope becomes positive, in practice it is rendered ineffective due to straggling. Cooling of all six phase-space dimensions is nevertheless required for a muon collider of useful luminosity. It is accomplished by the use of longitudinal–transverse emittance exchange, illustrated schematically in Fig. 3. A dipole field is employed to create dispersion. A wedge absorber can then be used to compensate for the beam momentum spread, reducing the longitudinal emittance at the expense of a wider spread in transverse position. It should be noted that the process can be exploited in either direction. In current muon collider designs, (forward) emittance exchange enables 6D cooling, and *reverse* emittance exchange is employed after 6D cooling, in order to reduce transverse emittance at the expense of longitudinal and further boost the luminosity (Fig. 4). (This is found to work better than attempting to tune the degree of 6D-channel emittance exchange to approach the desired final emittance directly.)

[2] Analogous to beam cooling by synchrotron radiation, in which energy loss provides cooling, while heating is caused by quantum fluctuations.

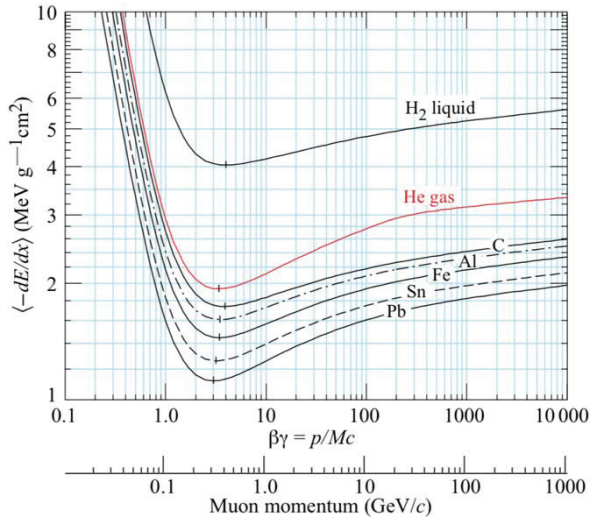

Figure 2: Ionization energy-loss rate vs. momentum (from [9]).

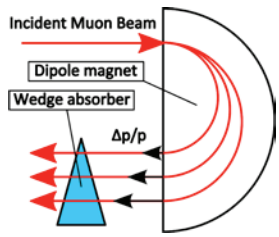

Figure 3: Principle of emittance exchange.

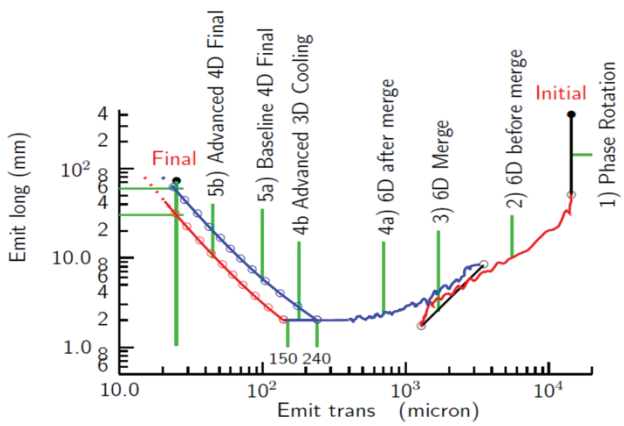

Figure 4: Emittance trajectory followed in a representative muon collider cooling design [21].

MICE

While the physics of Eq. 1 is well established, poorly modeled tails of distributions, as well as engineering limitations, could have important impact on ionization cooling-channel cost and performance. An initiative was therefore undertaken to build and test a realistic section of cooling channel: the international Muon Ionization Cooling Experiment (MICE) [22]; one component of the MICE program was to precisely measure the absorber material properties (dE/dx and multiple scattering distributions) that determine the performance of ionization cooling. Ionization cooling channels are tightly packed assemblies with

ISBN: 978-3-95450-218-9 ISSN: 2226-0374 doi:10.18429/JACoW-COOL2019-TUY02

liquid hydrogen, superconducting magnets, and high-gradient normal-conducting RF cavities in close proximity and concomitant safety issues with which little previous experience was available. Moreover, the cooling effect of the $\mathcal{O}(10^3)$ ionization cooling cells required to reach collider luminosities of interest might be degraded by poorly measured tails of the energy-loss and multiple-scattering distributions. An experimental demonstration was thus deemed essential to further progress.

MICE was proposed as a test of one lattice cell of the Feasibility Study II [23] transverse cooling channel (Fig. 5a). Being limited for cost reasons to an $\mathcal{O}(10\%)$ emittance reduction, it was conceived as a high-precision measure-

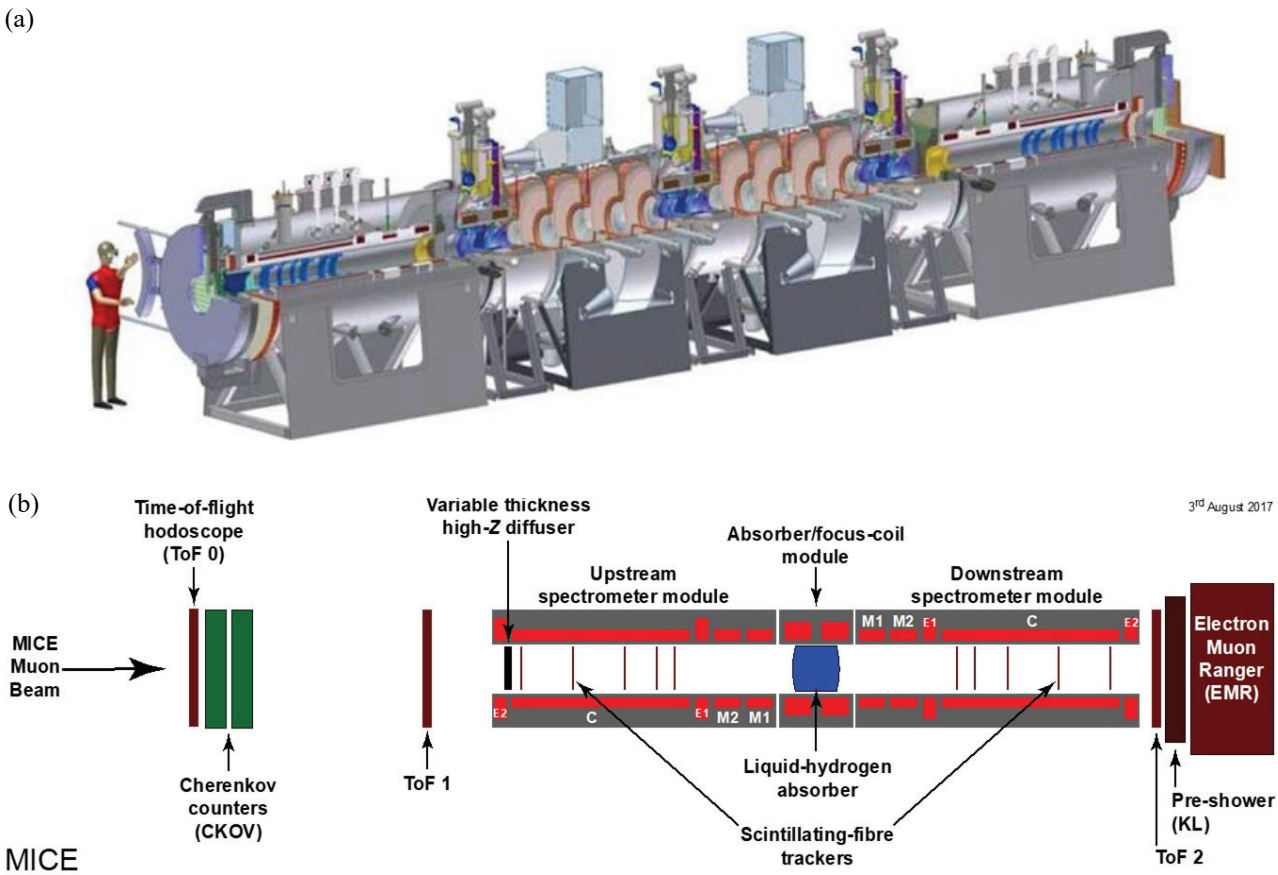

Figure 5: (a) MICE apparatus as originally proposed, with 3 absorbers and 8 RF cavities; (b) schematic of MICE apparatus as built; (c) installed in its hall off the RAL ISIS 800 MeV synchrotron, with solenoids surrounded by magnetic shielding.

ISBN: 978-3-95450-218-9 ISSN: 2226-0374 doi:10.18429/JACoW-COOL2019-TUY02

Figure 6: Photo of ½ of polyethylene-wedge absorber.

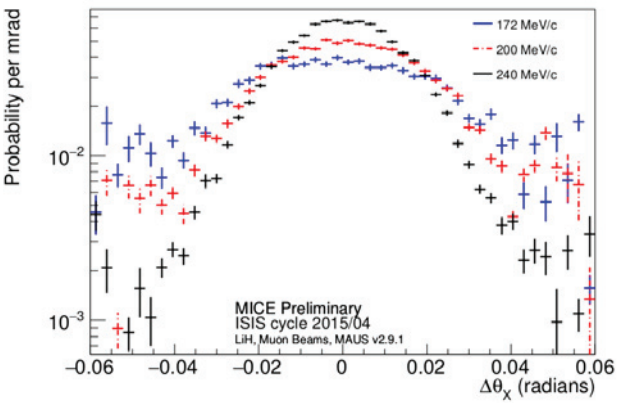

Figure 7: Deconvolution of observed scattering-angle distributions in x in three muon momentum settings.

ment of a low-intensity beam, via particle tracking carried out one muon at a time, with the unprecedented emittance resolution of 1‰. It was proposed by an international collaboration [22] and approved in 2003 at Rutherford Appleton Laboratory in the UK. After an extended design, construction, installation, and commissioning process, MICE recorded a substantial dataset (3.5×10^8 events) in 2016–17 with one absorber and no RF cavities. Various absorber materials (Table 1) were studied, including liquid hydrogen (LH_2) and lithium hydride (LiH), with a range of beam momenta and lattice focusing strength. Data were also taken with a 45° polyethylene wedge absorber (Fig. 6), in order to demonstrate emittance exchange.

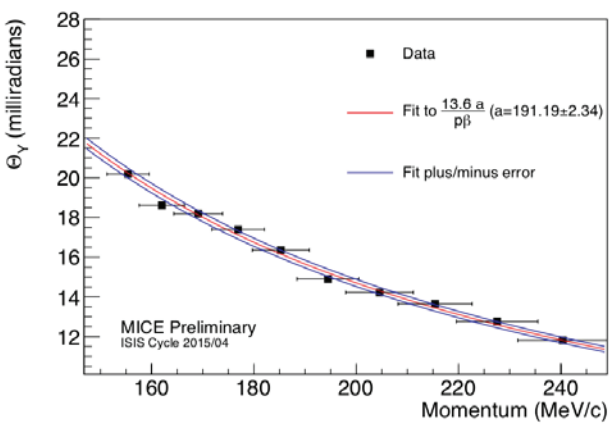

Figure 8: RMS of Gaussian fit to central ±40 mrad of deconvoluted scattering-angle distribution in y vs. muon momentum.

Table 1: Absorber Specifications

Absorber	Diameter (cm)	Thickness (cm)
LH_2	30	35
LiH	30	6.5
Polyethylene wedge	39	0 to 21 (5.2 on axis)

Study of Material Properties

Two approaches were taken to measuring multiple scattering: with solenoid fields off, and with them on. The field-off approach, with the advantages of analysis simplicity and straightforward systematics, is further along at present, and is the one presented here; the field-on measurement (once complete) should cover a wider range of scattering angle. Requirements on events included a reconstructed upstream track within the time of flight (TOF) and fiducial limits: that the measured time of flight between the TOF0 and TOF1 detector planes be consistent with that of a muon, and that the projection of the upstream track to the end of the downstream tracker lie within a 140 mm radius of the tracker center. The excellent resolution of the MICE TOF counters (≈55 ps) [24] allows reconstruction of the momentum of each muon, thus the analysis is carried out within 200 ps TOF bins. The TOF momentum is corrected to second order for the trajectory length of each muon and for energy loss in material (the TOF counters, tracker planes, helium, air, and windows). Data were taken with the (LiH) absorber removed or (LH_2) empty as well as with absorbers installed and full, allowing deconvolution of measurement resolution effects. Figure 7 shows the deconvolution results in x from three beam-momentum settings. Gaussian fits to the central ±40 mrad were performed independently in x and in y in each 200 ps TOF bin; results of the y fit are shown in Fig. 8 and are consistent with the results in x and with the expected $1/p\beta$ dependence. Study of systematic uncertainties is currently in progress. Results on the dE/dx distributions in LH_2 and LiH are also anticipated. A more detailed account appears in [25].

Cooling Results

Figure 9 illustrates how muons are selected, and pions and decay electrons rejected, by imposing two-dimensional cuts in the TOF–momentum plane. The first meas-

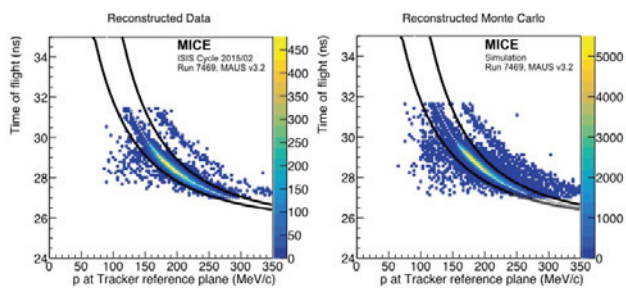

Figure 9: Observed (left) and simulated (right) time of flight vs. reconstructed momentum, showing bands of muons and (further up and to the right) pions. Curves show requirements used to select muons.

ISBN: 978-3-95450-218-9 ISSN: 2226-0374 doi:10.18429/JACoW-COOL2019-TUY02

urement of emittance using tracker information [26] is shown in Fig. 10, for data obtained in the nominal "3 mm·rad" emittance setting. While fair agreement with simulation is observed, the comparison is sensitive to poorly modelled features of pion production in 800 MeV proton-titanium interactions, thus precise agreement is not expected. Our cooling analysis, based on how the observed input emittance is modified by passage through absorbers, is insensitive to such modeling discrepancies.

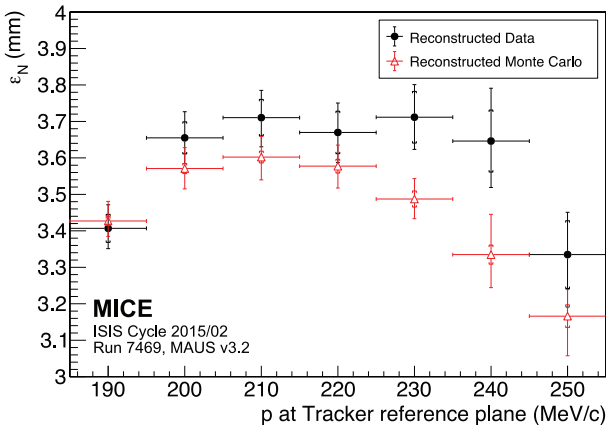

Figure 10: Measured input emittance vs. momentum [26].

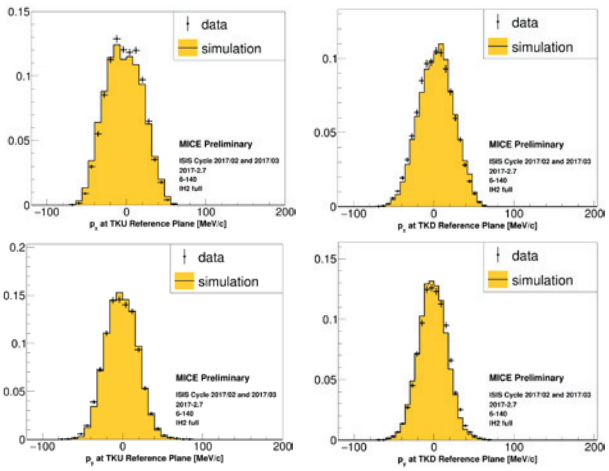

Figure 11: Comparison of observed and simulated (top) p_x and (bottom) p_y distributions, (left) upstream and (right) downstream of LH_2 absorber in 6 mm, 140 MeV/c sample.

In Fig. 11 the horizontal and vertical momentum-component distributions upstream and downstream of the LH_2 absorber are compared for the "6-140" data sample (i.e., nominal input emittance 6 mm·rad, nominal momentum 140 MeV/c). Cooling (narrowing of the transverse-momentum distributions) by a small amount is qualitatively apparent. To make the point more quantitative, Fig. 12 compares the observed distributions of single-particle amplitude (transverse distance from the beam centroid, measured in emittance units) upstream and downstream of the absorber for both the 6-140 and 10-140 datasets. Due to cost-saving compromises made during MICE construction, the beam transmission through the cooling cell was limited at large amplitude by apertures; furthermore, as is not uncommon, the beam at large amplitude was not well described by a Gaussian. For these reasons, the usual beam-quality figure of merit—total bunch RMS emittance—is not so useful. Thanks to the MICE single-particle measurement capability, the crucial behavior at and near the core of the beam is nevertheless clearly observable: with no absorber the phase-space density near the core is seen to decrease from upstream to downstream, while with either absorber in, it increases; this is the hallmark of cooling.

Figure 13 shows the cumulative ratio vs. amplitude of the number of muons downstream to that upstream of the absorber, again indicative of the change in phase-space density in the core of the beam. With no absorber, the density at the beam core slightly decreases. For both the LH_2 and LiH absorbers, a clear increase in core density is seen for both input-beam emittances.

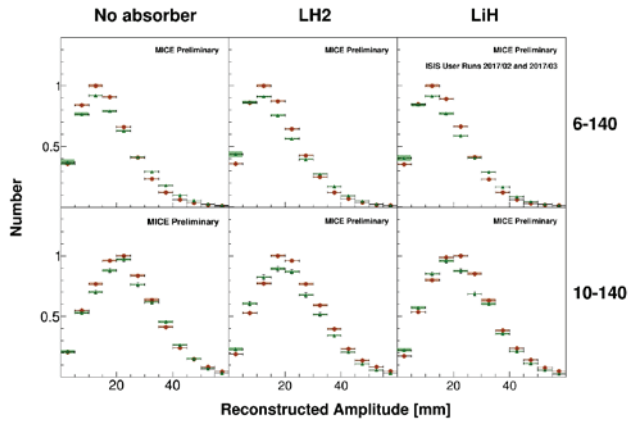

Figure 12: Comparison of upstream (red) and downstream (green) amplitude distributions without and with LH_2 and LiH absorbers for 6-140 and 10-140 datasets.

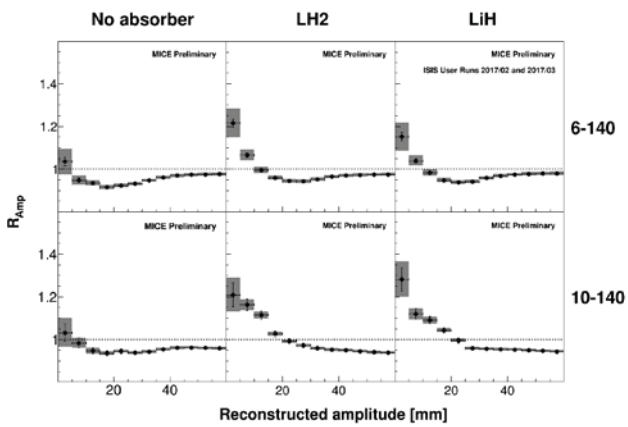

Figure 13: Cumulative ratios of downstream to upstream amplitude distributions without and with LH_2 and LiH absorbers for 6-140 and 10-140 datasets.

ISBN: 978-3-95450-218-9 ISSN: 2226-0374 doi:10.18429/JACoW-COOL2019-TUY02

CONCLUSION

The MICE Collaboration has recorded a substantial dataset with which to demonstrate muon ionization cooling and is well on its way to accomplishing its goals. Clear evidence of transverse ionization cooling has been presented. A more conclusive analysis including extensive discussion of systematics will appear in a future paper [27].

ACKNOWLEDGEMENTS

One of us (D.M.K.) gratefully acknowledges the kind hospitality experienced at the Budker Institute of Nuclear Physics.

REFERENCES

[1] R. Palmer, "Muon Colliders," *Rev. Accel. Sci. Tech*. 7 (2014) 137.

[2] D. Neuffer and V. Shiltsev, "On the feasibility of a pulsed 14 TeV c.m.e. muon collider in the LHC tunnel," *JINST* 13 (2018) T10003.

[3] D. Neuffer, M. Palmer, Y. Alexahin, C. Ankenbrandt, J. P. Delahaye, "A muon collider as a Higgs factory," in *Proc. of IPAC2013*, Shanghai, China, May 2013, paper TUPFI056.

[4] S. Geer, "Neutrino beams from muon storage rings: Characteristics and physics potential," *Phys. Rev. D* 57, 6989 (1998); ibid. 59, 039903E (1999).

[5] C. Albright *et al*., "Physics at a Neutrino Factory," FERMILAB-FN-0692, May 2000, hep-ex/0008064.

[6] M. Apollonio *et al*., "Oscillation Physics with a Neutrino Factory," CERN-TH-2002-208 Oct. 2002.

[7] A. Bandyopadhyay *et al*., "Physics at a future Neutrino Factory and super-beam facility," *Rep. Prog. Phys.* 72, 106201 (2009), arXiv:0802.4023 [physics.acc-ph].

[8] M. Lindner, "The physics potential of future long baseline neutrino oscillation experiments," in *Neutrino Mass*, G. Altarelli, K. Winter, Eds., *Springer Tracts in Modern Physics* 190, 209, 2003.

[9] The ISS Accelerator Working Group, "Accelerator design concept for future neutrino facilities," *JINST* 4, P07001 2009.

[10] S. Choubey *et al*. (IDS-NF Collaboration), "International Design Study for the Neutrino Factory, Interim Design Report," arXiv:1112.2853 [hep-ex] Mar. 2011.

[11] J. P. Delahaye *et al*., "Muon Colliders" (Input to the European Particle Physics Strategy Update), arXiv:1901.06150 [physics.acc-ph] 2019.

[12] D. M. Kaplan, "Muon cooling, muon colliders, and the mice experiment," in *Proc. COOL2013*, paper MOAM2HA01.

[13] D. M. Kaplan, "Muon Colliders, Neutrino Factories, and Results from the MICE Experiment," in *Proc. CAARI 2018*, *AIP Conf. Proc.* 2160, 040011 (2019).

[14] Y. M. Ado, V. I. Balbekov, "Use of ionization friction in the storage of heavy particles," *Soviet At. Energ*. 31(1) 40 (1971), English translation in *Atomic Energy* (Springer) 31(1) 731, http://www.springerlink.com/content/v766810126338571/.

[15] D. Neuffer, in *Advanced Accelerator Concepts, AIP Conf. Proc.* 156, 201 (1987).

[16] D. V. Neuffer, R. B. Palmer, "A high-energy high-luminosity μ+-μ− collider," in *Proc. 1994 Eur. Part. Accel. Conf. (EPAC94)*, p. 52.

[17] R. C. Fernow, J. C. Gallardo, *Phys. Rev. E* 52, 1039 (1995).

[18] C. M. Ankenbrandt *et al*., "Status of Muon Collider Research and Development and Future Plans," *Phys. Rev. ST Accel. Beams* 2, 081001 (1999).

[19] D. Neuffer, "μ+ μ− Colliders," Yellow Report CERN-99-12 (1999).

[20] "Passage of Particles Through Matter," in M. Tanabashi *et al*. [Particle Data Group], *Phys. Rev. D* 98, 030001 (2018).

[21] D. Neuffer, H. Sayed, J. Acosta, T. Hart and D. Summers, "Final cooling for a high-energy high-luminosity lepton collider," *JINST* 12 (20187) T07003.

[22] G. Gregoire *et al*., "An International Muon Ionization Cooling Experiment (MICE)," Proposal to Rutherford Appleton Laboratory, http://mice.iit.edu/micenotes/public/pdf/MICE0021/MICE0021.pdf

[23] S. Ozaki *et al*., "Feasibility Study-II of a Muon-Based Neutrino Source," https://www.cap.bnl.gov/mumu/studyii/FS2-report.html, BNL-52623 (2001).

[24] R. Bertoni *et al*., "The Design and Commissioning of the MICE Upstream Time-of-Flight System," *Nucl. Instrum. Meth. A* 615 (2010) 14.

[25] D. M. Kaplan, J. C. Nugent, and P. Soler, "Recent Results from MICE on Multiple Coulomb Scattering and Energy Loss," in *Proc. COOL'19* (this workshop), paper TUB01.

[26] D. Adams *et al*. [MICE Collaboration], "First particle-by-particle measurement of emittance in the Muon Ionization Cooling Experiment," *Eur. Phys. J. C* 79 (2019) 257.

[27] M. Bogomilov *et al*. [MICE Collaboration], submitted for publication (2019).